Bioorganic & Medicinal Chemistry 19 (2011) 122–133

Contents lists available at ScienceDirect

Bioorganic & Medicinal Chemistry

journal homepage: www.elsevier.com/locate/bmc

Cholinergic and neuroprotective drugs for the treatment of Alzheimer and neuronal vascular diseases. II. Synthesis, biological assessment, and molecular modelling of new tacrine analogues from highly substituted 2-aminopyridine-3-carbonitriles

Abdelouahid Samadi [a], Carolina Valderas [a], Cristóbal de los Ríos [b,c], Agatha Bastida [a], Mourad Chioua [a], Laura González-Lafuente [b], Inés Colmena [b], Luis Gandía [b], Alejandro Romero [b], Laura del Barrio [b], María D. Martín-de-Saavedra [b], Manuela G. López [b], Mercedes Villarroya [b], José Marco-Contelles [a,*]

[a] Laboratorio de Radicales Libres y Química Computacional (IQOG, CSIC), C/Juan de la Cierva 3, 28006 Madrid, Spain
[b] Instituto Teófilo Hernando, and Departamento de Farmacología y Terapéutica, Facultad de Medicina, Universidad Autónoma de Madrid, C/Arzobispo Morcillo 4, 28029 Madrid, Spain
[c] Departamento de Química Orgánica, Facultad de Farmacia, Universidad de Alcala, Ctra. Barcelona, Km. 33.5, 28817 Alcalá de Henares, Spain

ARTICLE INFO

Article history:
Received 17 September 2010
Revised 15 November 2010
Accepted 18 November 2010
Available online 26 November 2010

This manuscript is dedicated to Professor Antonio G. García on occasion of his 65th birthday

Keywords:
2-Aminopyridin-3-carbonitriles
Tacrine analogues
AChE
BuChE
Inhibition mechanism
Neuroprotection
Molecular modelling
Alzheimer's disease
Neuronal cerebrovascular diseases

ABSTRACT

The synthesis, biological assessment, and molecular modelling of new tacrine analogues **11**–**22** is described. Compounds **11**–**22** have been obtained by Friedländer-type reaction of 2-aminopyridine-3-carbonitriles **1**–**10** with cyclohexanone or 1-benzyl-4-piperidone. The biological evaluation showed that some of these molecules were good AChE inhibitors, in the nanomolar range, and quite selective regarding the inhibition of BuChE, the most potent being 5-amino-2-(dimethylamino)-6,7,8,9-tetrahydrobenzo[1,8-*b*]-naphthyridine-3-carbonitrile (**11**) [IC_{50} (EeAChE: 14 nM); IC_{50} (eqBuChE: 5.2 μM]. Kinetic studies on the easily available and potent anticholinesterasic compound 5-amino-2-(methoxy)-6,7,8,9-tetrahydrobenzo[1,8-*b*]-naphthyridine-3-carbonitrile (**16**) [IC_{50} (EeAChE: 64 nM); IC_{50} (eqBuChE: 9.6 μM] showed that this compound is a mixed-type inhibitor (K_i = 69.2 nM) of EeAChE. Molecular modelling on inhibitor **16** confirms that this compound, as expected and similarly to tacrine, binds at the catalytic active site of EeAChE. The neuroprotective profile of molecules **11**–**22** has been investigated in SH-SY5Y neuroblastoma cells stressed with a mixture of oligomycin-A/rotenone. Compound **16** was also able to rescue by 50% cell death induced by okadaic acid in SH-SY5Y cells. From these results we conclude that the neuroprotective profile of these molecules is moderate, the most potent being compounds **12** and **17** which reduced cell death by 29%. Compound **16** does not affect ACh- nor K^+-induced calcium signals in bovine chromaffin cells. Consequently, tacrine analogues **11**–**22** can be considered attractive therapeutic molecules on two key pharmacological targets playing key roles in the progression of Alzheimer, that is, cholinergic dysfunction and oxidative stress, as well as in neuronal cerebrovascular diseases.

1. Introduction

Alzheimer's disease (AD) is an age-related neurodegenerative process characterized by a progressive loss of cognitive abilities, such as memory, language skills, attention, disorientation, and depression.[1] Although the etiology of AD is still poorly understood, several factors such as amyloid-β (Aβ)[2] deposits, τ-protein aggregation, oxidative stress, or low levels of acetylcholine[3] are thought to play significant roles in the pathology of the disease.[4] In spite of the enormous research effort, an efficient strategy for designing new drugs for the treatment of AD is still lacking.

The cholinergic theory[1] suggests that the selective loss of cholinergic neurons in AD results in a deficit of acetylcholine (ACh) in specific regions of the brain that mediate learning and memory functions.[5] Consequently, three acetylcholinesterase (AChE) inhibitors have been approved for commercial use. Thus, donepezil, rivastigmine, and galantamine are known to improve AD symptoms by inhibiting AChE, that is, the enzyme responsible for the hydrolysis of ACh, thereby rising the levels of ACh in the synaptic cleft.[6] Recently, a renewed interest for AChE inhibitors has been stimulated by the potential role of AChE in accelerating the formation of amyloid fibrils in the brain and forming stable complexes with Aβ.[7] This role involves the peripheral anionic binding site (PAS) of AChE, as noted by the fact that propidium iodide, a potent acetylcholinesterase inhibitor (AChEI) agent binding specifically to the

* Corresponding author. Tel.: +34 91 5622900; fax: +34 91 5644853.
E-mail address: iqoc21@iqog.csic.es (J. Marco-Contelles).

0968-0896/$ - see front matter © 2010 Elsevier Ltd. All rights reserved.
doi:10.1016/j.bmc.2010.11.040

PAS, affects Aβ aggregation in vitro, whereas other catalytic active site (CAS) inhibitors, such as tacrine, have not a similar effect.[8]

The multifactorial nature of AD supports new therapeutic strategies. The most current innovative therapeutic approach is based on the 'one molecule, multiple targets' paradigm.[9–13] Thus, the multipotent approach[14] includes novel tacrine-melatonin hybrids,[15] dual inhibitors of AChE and monoamine oxidase[16] or serotonin transporters,[17] potent cholinesterase inhibitors with antioxidant and neuroprotective properties,[18] gallamine-tacrine hybrids binding at cholinesterases and M_2 muscarinic receptors,[19] or AChE inhibitors and tau-hyperphosphorylation regulators.[20]

Based on these precedents, some years ago we have embarked in a project focused on the synthesis of multipotent molecules able to improve the cholinergic neurotransmission, showing also L-type Ca^{2+} channel antagonist effects. As a result, we have reported the chemistry and pharmacology of *tacripyrines*,[21a] as potent, selective (AChE vs BuChE), and mixed-type inhibitors, binding preferentially at the PAS of AChE, interfering with the Aβ pro-aggregating effect of human AChE (hAChE), and the self-aggregation of $A\beta_{1-42}$; in addition, tacripyrines were potent Ca^{2+} antagonists, pass through blood–brain barrier, and display neuroprotective and antioxidant properties.[21a]

In this context, we have recently described the synthesis, molecular modelling and pharmacological analysis of new, simple, and readily available 2-aminopyridine-3,5-dicarbonitriles (**I**), and 2-chloropyridine-3,5-dicarbonitriles (**II**) (Chart 1).[21b] From this work, we concluded that these molecules were modest inhibitors of AChE and butyrylcholinesterase (BuChE), in the micromolar range. No clear structure–activity relationship (SAR) could be obtained from these data; but apparently, compounds bearing small groups such as *N*,*N*′-dimethylamino or the pyrrolidine, regardless of the presence of 2-amino or 6-chloro substituents at the pyridine ring, preferentially inhibited AChE. The neuroprotective profile of these molecules was also investigated showing neuroprotection with values around 30% in SH-SY5Y neuroblastoma cells stressed with a mixture of oligomycin-A/rotenone.

Based on these results, and in order to improve the observed cholinergic and neuroprotective profile, we considered that the corresponding tacrine analogues **III**, synthesized from the most potent and neuroprotective molecules of the type **I** (Chart 1), could therefore be attractive synthetic targets that would deserve to be prepared and investigated.

Thus, in this manuscript we describe the successful accomplishment of these objectives, reporting the chemistry and pharmacology of the new tacrine analogues **11–22** derived from the pharmacologically active 2-aminopyridine-3,5-dicarbonitriles **1–10** (Table 1) of family **I** (Chart 1).[21b]

2. Results and discussion

2.1. Chemistry

We have synthesized the differently substituted tacrine analogues **11–20** by reacting the corresponding 2-aminopyridine-3,5-dicarbonitriles **1–10** with cyclohexanone in Friedländer-type reaction conditions (Scheme 1).[22] Microwave irradiation was preferred[23] because in some instances (see Table 1, entries f and i), classical heating conditions gave lower chemical yields. Table 1 shows the structure of the 2-aminopyridine-3,5-dicarbonitriles **1**, **4**, **5**, **9** and **10**,[21b] and the structure of known precursors **2**,[24] **3**,[24] **6**,[25] **7**,[26] and **8**,[27] synthesized as described, as well as the structure of the resulting tacrine analogues with their chemical yields. We have also prepared tacrines **21** and **22** (Table 1) by reacting both 2-aminopyridine-3,5-dicarbonitriles **6**[25] and **9**[21b] with 1-benzyl-4-piperidone, in modified Friedländer-type reaction conditions using trimethylsilyl triflate as promotor, and ethyl acetate as solvent (Scheme 1).[28] All new compounds showed analytical and

Table 1
Synthesis of tacrine analogues **11–22**

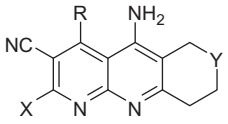

Entry	Precursor of general structure I [ref]	Product of general structure III	R	X	Y	Yield % by MW irradiation (classical heating)
a	**1**[21b]	**11**	H	Me_2N	CH_2	72
b	**2**[24]	**12**	H		CH_2	98
c	**3**[24]	**13**	H		CH_2	91
d	**4**[21b]	**14**	H	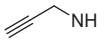	CH_2	78
e	**5**[21b]	**15**	Ph	Me_2N	CH_2	47
f	**6**[25]	**16**	H	MeO	CH_2	95 (51)
g	**7**[26]	**17**	H	EtO	CH_2	92
h	**8**[27]	**18**	Ph	MeO	CH_2	67
i	**9**[21b]	**19**	H	Cl	CH_2	30 (9)
j	**10**[21b]	**20**	Ph	Cl	CH_2	20
k	**6**[25]	**21**	H	MeO	NBn	81
l	**9**[21b]	**22**	H	Cl	NBn	54

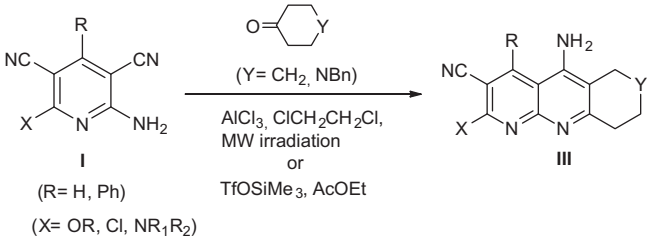

Scheme 1. Synthesis of tacrine analogues **III** by Friedländer-type reaction between 2-aminopyridine-3-carbonitriles **I** and either cyclohexanone or 1-benzyl-4-piperidone.

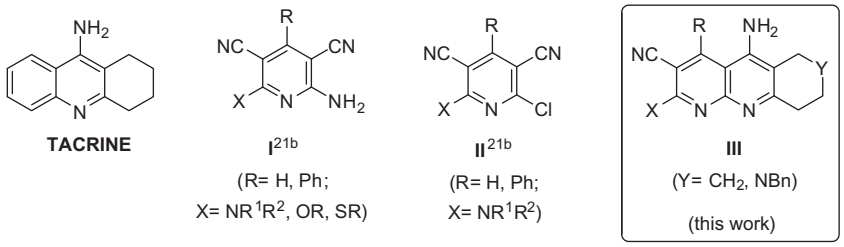

Chart 1. The structures of tacrine, 2-aminopyridine-3,5-dicarbonitriles (**I**), 2-chloropyridine-3,5-dicarbonitriles (**II**), and the new tacrine analogues (**III**).

Table 2
Inhibition of AChE from *Electrophorus electricus* (EeAChE) and bovine erythrocytes (beAChE), and horse serum BuChE (eqBuChE) by tacrine analogues **11**–**22**[a]

Entry	Product of general structure III	Structure	IC_{50} (μM)			Selectivity eqBuChE/EeAChE
			beAChE	EeAChE	eqBuChE	
a	**11**	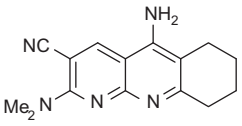	0.10 ± 0.02	0.014 ± 0.001	5.2 ± 0.4	371
b	**12**	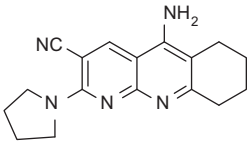	0.16 ± 0.02	0.043 ± 0.006	5.6 ± 0.3	130
c	**13**	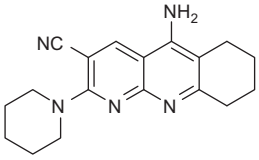	1.0 ± 0.1	0.025 ± 0.005	3.6 ± 0.2	144
d	**14**	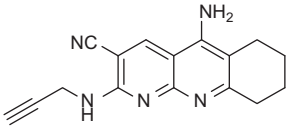	1.53 ± 0.04	0.030 ± 0.003	2.6 ± 0.3	87
e	**15**	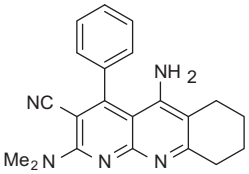	4.4 ± 0.3	0.09 ± 0.02	7.5 ± 0.1	83
f	**16**	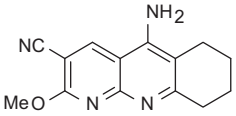	1.6 ± 0.4	0.06 ± 0.01	9.6 ± 0.6	160
g	**17**	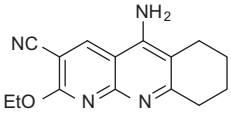	1.0 ± 0.2	0.050 ± 0.001	>30	>600
h	**18**	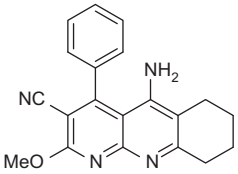	5 ± 1	0.08 ± 0.01	5.1 ± 0.9	64
i	**19**	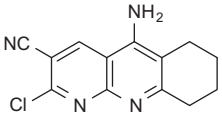	>100	5.0 ± 0.4	>30	>6
j	**20**	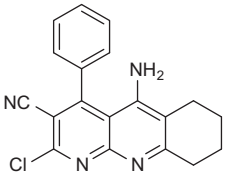	>100	>30	>30	1
k	**21**	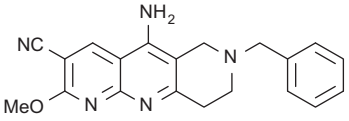	5 ± 1	0.35 ± 0.04	>100	>286

Table 2 (*continued*)

Entry	Product of general structure III	Structure	IC_{50} (μM)			Selectivity eqBuChE/EeAChE
			beAChE	EeAChE	eqBuChE	
l	**22**	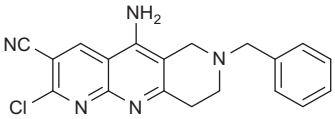	>100	0.35 ± 0.09	>100	>286
m	Tacrine	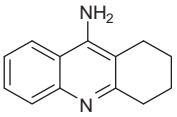	0.109 ± 0.03	0.027 ± 0.002	0.0052 ± 0.0002	0.19

[a] Data are expressed as mean ± SEM of quadruplicates of at least three independent experiments.

spectroscopic data in good agreement with their structures (see Section 4).

2.2. Pharmacology

2.2.1. Anticholinesterasic activity

2.2.1.1. AChE/BuChE inhibitory activity. Tacrine analogues **11**–**22** were evaluated as inhibitors of AChE from *Electrophorus electricus* (Ee) and from bovine erythrocytes (be), and BuChE from horse serum (eq), according to Ellman's protocol.[29] The results are shown in Table 2. From the IC_{50} values, we conclude that molecules **11**–**18** are good EeAChE inhibitors, and quite selective regarding to the inhibition of eqBuChE, the most potent being 5-amino-2-(dimethylamino)-6,7,8,9-tetrahydrobenzo[1,8-*b*]-naphthyridine-3-carbonitrile (**11**) [IC_{50} (AChE: 14 nM); IC_{50} (BuChE: 5.2 μM)]. Note that compared with tacrine, inhibitor **11** had similar AChE inhibition profile, but it is less potent BuChE inhibitor. Regarding eqBuChE, the most potent inhibitor was tacrine analogue **14** (IC_{50} = 2.6 ± 0.3 μM).

Structure–activity relationship (SAR) studies show us, firstly, that the presence of either an hydrogen or a phenyl ring at C-4 has no significant effect on the inhibition of eqBuChE, as IC_{50} values for inhibitors **11**:**15**, or **16**:**18**, bearing a similar dimethylamino (NMe_2), or a methoxy (OMe) substituent at C-2, respectively. Removal of the phenyl ring significantly improved AChE inhibition only in the case of compound **11**, as compared with compound **15**. Compounds **11**–**18**, bearing an electron-donating group at C2, were nanomolar-ranged AChEI, being C2-amino-substituted compounds **11**–**15** slightly more potent than C2-alkoxy-substituted inhibitors **16**–**18**. AChE inhibition was noticeably affected by the size of the N2-alkyl substitution, as seen in compounds **11**–**15**. The shortest *N*-methyl-substituted compound **11** inhibited AChE better than compounds having larger alkyl chains at N2. Note also that the size of the alkoxy-substituent has no significant influence on the AChE inhibition, as the ethoxy-substituted derivative **17** showed a similar IC_{50} compared to the methoxy-substituted derivatives **16** or **18**. Conversely, and for the inhibition of eqBuChE, on going from methoxytacrine **16** to ethoxytacrine **17** the AChE activity is lost, but recovered, in the same range, when a phenyl ring is located at C4 as in inhibitor **18**. Overall, the observed eqBuChE inhibition for molecules **11**–**20** ranged between 2.6 and >30 μM. The incorporation of an electron withdrawing substituent, such as a chlorine atom, at C-2, resulted in a dramatic loss of cholinesterase activity. Finally, it has been observed that the change of the methylene group (CH_2) at C-7 in inhibitors **16** and **19** by an NBn (*N*-benzyl) group in inhibitors **21** and **22**, respectively, augmented AChE selectivity. Compared with compound **21**, inhibitor **16**, bearing also a methoxy group at C-2, was 5.8-fold more active; but interestingly, inhibitor **19** was found 14-fold less potent than **22** for the inhibition of EeAChE, bearing both compounds a chlorine atom at C-2.

Inhibition experiments using beAChE showed IC_{50} data mainly in the micromolar range, being compound **11** the best inhibitor, with an IC_{50} of 0.1 μM. Hence, these compounds were much more active inhibiting eeAChE than beAChE. The reason for this enzymatic selectivity could be due to some structural differences, such as eeAChE being a flexible tetramer,[30] while mammal erythrocytes AChE is presented in globular dimers,[31] or because they show different rate of glycosylation.[32] Although some authors have not found any differences in the catalytic behavior of both enzymes, there are several papers describing a differential inhibitory activity for eeAChE and mammal erythrocytes AChE with physostigmine, organophosphorus, and carbamate analogues.[33] Otherwise, the fact that these compounds were better inhibitors of eeAChE, an enzyme structurally related to the brain enzyme,[34] than the peripheral bovine erythrocyte AChE could be beneficial for a potential further clinical development, taking into account that many of the side effects of AChE inhibitors are due to the inhibition of the peripheral enzyme.

2.2.1.2. Kinetic analysis for the EeAChE inhibition. Based on the previous results, and taking into account the availability based on the high chemical yield obtained in its synthesis, and the ChE inhibition profile, due to the potency and selectivity, we selected inhibitor 5-amino-2-(methyloxy)-6,7,8,9-tetrahydrobenzo[1,8-*b*]-naphthyridine-3-carbonitrile (**16**) [IC_{50} (EeAChE: 64 nM); IC_{50} (eqBuChE: 9.6 ± 0.6 mM] to carry out the pertinent kinetic analysis to determine the K_i and the mechanism for the inhibition of EeAChE. Among the most active AChEI, compound **16** presented the smallest substituent at C2. In addition, inhibitor **16** has been isolated in high chemical yield, and although shows inhibitory potency (IC_{50}) slightly lower than other tacrine analogues (see for instance, compounds **12**, **13** and **17**), these values are in the same order of magnitude. The type of inhibition was elucidated from the analysis of Lineweaver–Burk reciprocal plots (Fig. 1) showing increasing slopes (lower V_{max}) and slightly increasing intercepts (higher K_m) with higher inhibitory concentration. The graphical analysis of steady-state inhibition data for compound **16** is shown in Figure 1, where plots of different inhibitor concentrations almost intersect in *x*-axis. This would suggest a non-competitive inhibition, but scaling down the Lineweaver–Burk plot we can see lines converging just above the *x*-axis. This suggests a mixed-type inhibition.[35] This type of inhibition was also confirmed by the fact that the resulting K_i value, estimated from the slopes of double reciprocal plots versus compound **16** concentrations was 69.2 nM, while the K_i value, estimated from the intercepts in *y*-axis of double reciprocal plots versus compound **16** concentrations was 143 nM.

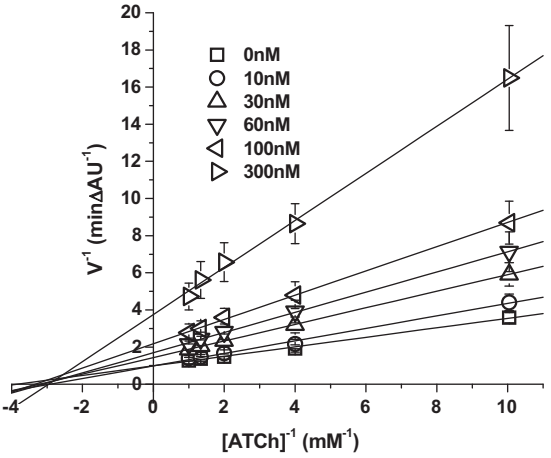

Figure 1. Steady-state inhibition of AChE hydrolysis of acetylthiocholine (ATCh) by compound **16**. Lineweaver–Burk reciprocal plots of initial velocity and substrate concentrations (0.1–1 mM) are presented. Lines were derived from a weighted least-squares analysis of data.

2.2.1.3. Molecular modelling. Next, a molecular modelling study was performed in order to determine the binding mode of the ligand **16** to the AChE from *Torpedo californica*. Docking analysis was performed with AutoDock 4.0 program.[36] A box encompassing both the CAS and the PAS site was defined for the exploration of possible binding modes in the enzyme. Two different protonation states were proposed for compound **16**, the mode **I**, without protonation at pyridine ring C, and **II**, with it. For both states, the results showed that the ligand was exclusively docked at the CAS site. The putative binding mode is analogous to that found in the crystallographic complex of tacrine bounded at the CAS site of AChE (Fig. 2). To validate and test the stability of the proposed binding mode (**I** and **II**) obtained by docking, molecular dynamics (MD) simulation have been carried out. Compound **16** (mode **I** and **II**) remain docked along the simulations within the proposed binding pocket and retained its starting conformation (rmsd <0.5 Å for all non-hydrogen atoms) (see Figs. 3 and 4). The inspection of the van der Walls contributions of individual residues to the binding energy reveals that major interactions arise from Trp84, Asp85, Ser 200, Phe330, Tyr 334, Trp423, and His440.

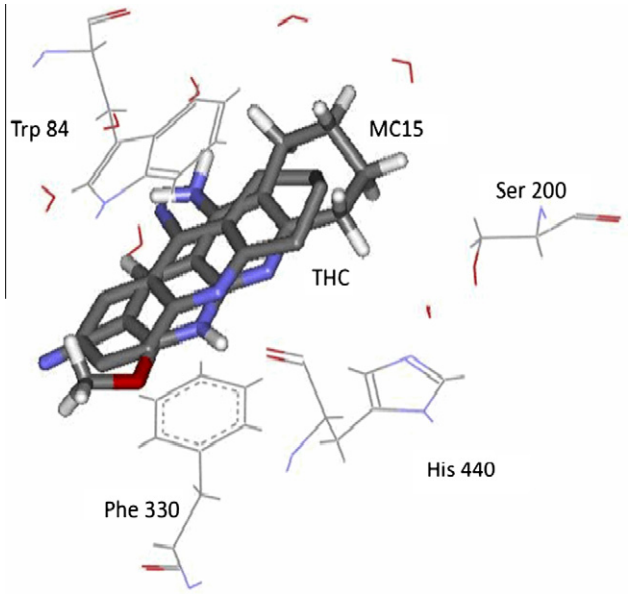

Figure 2. Binding mode of **16** and THC to AChE after docking in the CAS site. Some relevant residues are shown as sticks. Ligands are displayed as sticks with carbon atoms in gray, (O, red and N, blue). Water molecules are represent as red sticks.

In summary, the calculations suggest that the ligand is successfully docked in the CAS site of the AChE which shows a high stability, as supported by MD simulations.

2.2.2. Neuroprotection of compounds 11–22 against rotenone/oligomycin-A-induced cell death

The exposure of SH-SY5Y cells to a mixture of rotenone plus oligomycin (Rot/Olig) constitutes a good model of oxidative stress having its origin in mitochondria.[37] Rotenone blocks complex I of mitochondrial electron transport chain and oligomycin-A inhibits complex V, thus disrupting ATP synthesis; they elicit neurotoxicity and allow the evaluation of potential neuroprotective drugs used to treat AD patients, which inhibit AChE, such as galanthamine, donepezil and rivastigmine. The results shown in Table 3 indicate that compounds **11–22** showed modest neuroprotective effect against oxidative stress, and in the same range of the well known reference antioxidant *N*-acetylcysteine (NAC).[38] Compounds **12** and **17** induced a protection of 29%, while tacrine analogues **22**, **13**, **14** and **16** protected by 20% (Table 3). However, no clear SAR has been found in this series of compounds to evaluate or predict more new potent neuroprotective agents.

2.2.3. Effect of compound 16 on cells treated with okadaic acid

The Ser/Thr phosphatase inhibitor okadaic acid reproduces a characteristic of the pathology of AD, that is, τ-protein phosphorylation in different in vivo[39] and in vitro[40] models, such as in the human neuroblastoma cell line SH-SY5Y,[39a,41] which is the mechanism giving rise to neurofibrillary tangles (NFTs). Thus, it is accepted that okadaic acid-induced toxicity is a good model for the neuronal death occurring in Alzheimeŕs disease and that is linked to tau-hyperphosphorylation.[20a]

Cells exposed to okadaic acid 30 nM in the absence of the compound showed 61 ± 3% cell death with respect to control cells (8.0 ± 0.1%), measured as % of LDH release. Compound **16** was able to significantly reduce cell death induced by okadaic acid from 0.1 to 1 μM; with a maximum reduction of LDH release 0.1 μM (49% respect to control). There were no statistically significant differences between 0.1 and 1 μM. Higher doses were not neuroprotective. Galanthamine, used as reference, protected SH-SY5Y cells by 67% at 0.3 μM (data not shown).[41b]

2.2.4. Analysis of compound 16 as nAChR blocker or as a voltage-dependent calcium channels antagonist

As previously documented, and discussed,[20,21] the ability of our tacrine analogues to act as Ca^{2+} channels blockers to prevent apoptosis and neuronal death, was of interest in the search for drugs for AD. To evaluate these pharmacological activities, we have selected again compound **16**.

To explore the potential of compound **16** as putative nicotinic receptors (nAChR) blocker or as a voltage-dependent calcium channels antagonist, changes in cytosolic Ca^{2+} signals ($[Ca^{2+}]_c$) elicited by application of the nAChR agonist acetylcholine (ACh, 100 μM) or depolarizing solutions (70 mM K^+) were evaluated in bovine chromaffin cell populations. Figure 5A shows a representative experiment carried out in bovine chromaffin cells in the absence (control) and in the presence of 10 μM of inhibitor **16**. The application of ACh (left panel) or K^+ (right panel) elicited a sharp increase in $[Ca^{2+}]_c$ that reached a plateau and then tended to slowly decline along the 40 s of the recording. Incubation of the cells with compound **16** (10 μM) did not significantly affect the $[Ca^{2+}]_c$ signal. Figure 5B shows average data obtained by using this type of protocol in cells from four different cell cultures and six different concentrations of the compound (0.3, 1, 3, 10, 30, and 100 μM); No

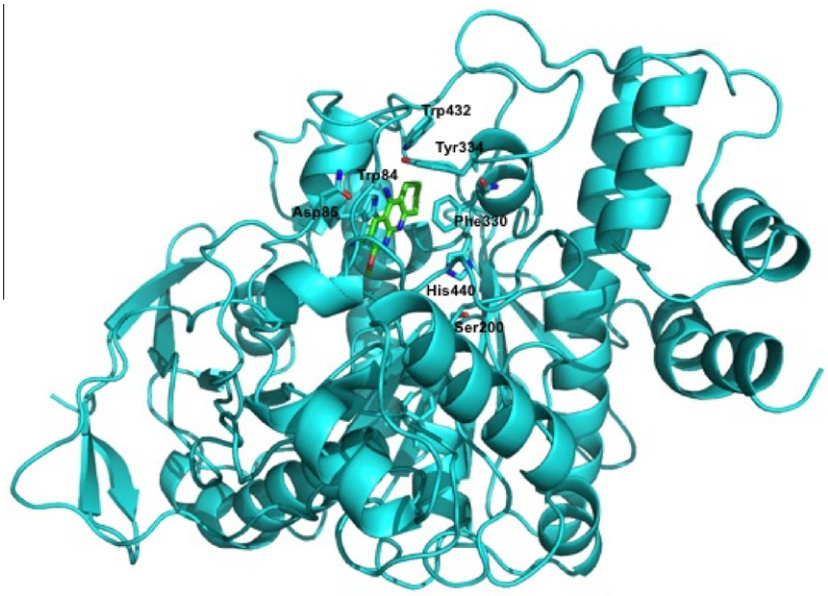

Figure 3. Binding mode of compound **16** to AChE after docking and MD simulation. The C (alpha) traces of the enzyme are displayed as a ribbon. Some relevant residues are shown as sticks. Ligand is displayed as sticks with carbon atoms in green.

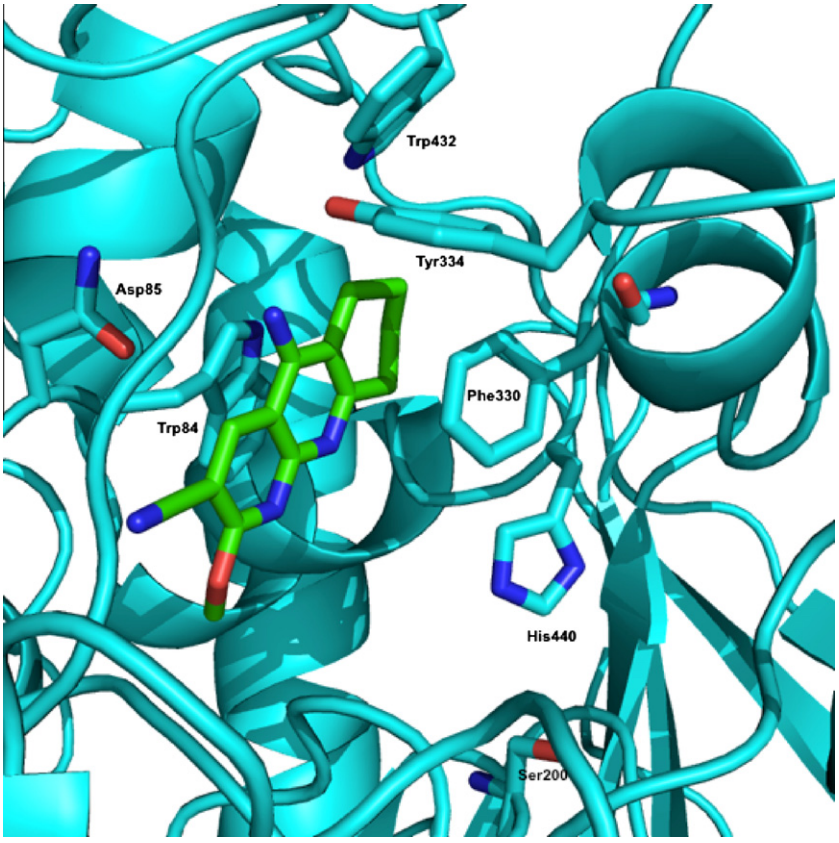

Figure 4. Representation of the binding mode of the ligand **16** in the CAS predicted by the docking and MD simulation. Relevant residues are shown as sticks and colour by atoms (C, blue). The residues forming the hydrophobic pocket belong to the active site (Trp 84, Trp 334, Phe 330, His 440, Ser 200 and Asp 85). Ligand is colour by atoms (C, green).

clear effects on either the ACh-elicited (left panel) nor the K^+-elicited (right panel) $[Ca^{2+}]_c$ signal was observed. These results suggest that this compound does not behave as a nAChR antagonist nor as a voltage-dependent calcium channel antagonist. Lack of nicotinic antagonism of **16** is considered beneficial, as nAChRs antagonists have been described to impair memory and cognitive functions. By contrast, Ca^{2+} channels blockers have shown neuroprotection in different models of neurodegeneration. Otherwise, the loss of

Table 3
Neuroprotection induced by the tacrine analogues (**11**–**22**) (1 μM) in human neuroblastoma cells stressed with a mixture of rotenone/oligomycin-A[a]

Entry	Product of general structure III	Structure	% Protection
a	**11**	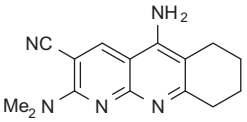	6
b	**12**	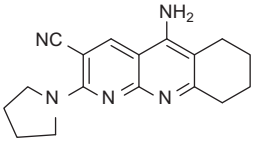	29
c	**13**	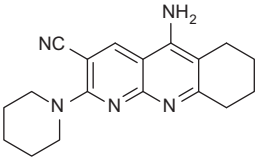	19
d	**14**	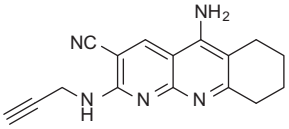	20
e	**15**	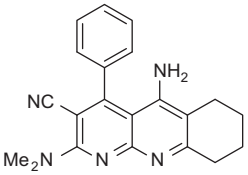	3
f	**16**	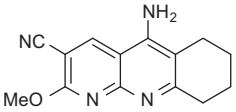	23
g	**17**	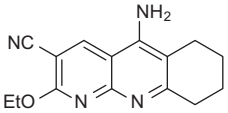	29
h	**18**	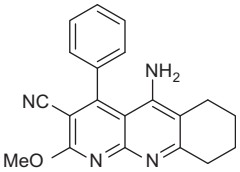	12
i	**19**	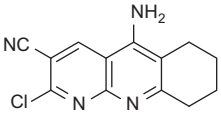	4
j	**20**	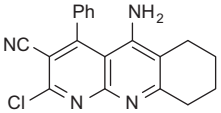	8
k	**21**	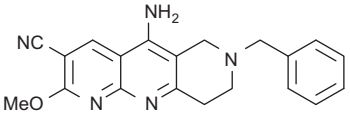	11
l	**22**	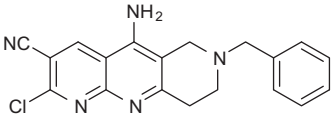	20
m	NAC		33

[a] The results are the averaged values, of at least three experiments, of percentages of MTT reduction compared to control in absence of drugs. NAC: *N*-acetylcysteine.

activity over Ca^{2+} channels has also been found in close analogues recently described by our group, which maintained a very interesting neuroprotective profile.[20a]

3. Conclusions

In this work, we have described the synthesis, biological assessment, and molecular modelling of new tacrine analogues **11–22**. Compounds **11–22** have been obtained by Friedländer-type reaction of 2-aminopyridine-3-carbonitriles **1–10** with cyclohexanone, as well as with 1-benzyl-4-piperidone for comparative purposes. The biological evaluation showed that some of these molecules were good AChE inhibitors, in the nanomolar range, and quite selective regarding the inhibition of BuChE, the most potent being 5-amino-2-(dimethylamino)-6,7,8,9-tetrahydrobenzo[1,8-*b*]-naphthyridine-3-carbonitrile (**11**). Kinetic studies on the easily available and potent anticholinesterasic compound 5-amino-2-(methoxy)-6,7,8,9-tetrahydrobenzo[1,8-*b*]-naphthyridine-3-carbonitrile (**16**) showed that this compound is a mixed-type inhibitor (K_i = 69.2 nM) of EeAChE. Molecular modelling on inhibitor **16** confirms that this compound, as expected, and similarly to tacrine, binds at the catalytic active site of AChE. The modest neuroprotective profile shown by molecules **11–22** has been investigated in SH-SY5Y neuroblastoma cells stressed with a mixture of oligomycin-A/rotenone. From these results we conclude that the neuroprotective profile of these molecules is rather moderate, the most potent being compounds **12** and **17** which reduced cell death by 29%. However, one of these molecules, compound **16**, was able to rescue by 50% cell death induced by okadaic acid in SH-SY5Y cells. Very interestingly, compound **16** does not affect ACh- nor K^+-induced calcium signals in bovine chromaffin cells.

To sum up, tacrine analogues **11–22** can be considered attractive therapeutic molecules on two key pharmacological receptors playing key roles in the progression of Alzheimer, that is, cholinergic dysfunction and oxidative stress, as well as in neuronal cerebrovascular diseases.

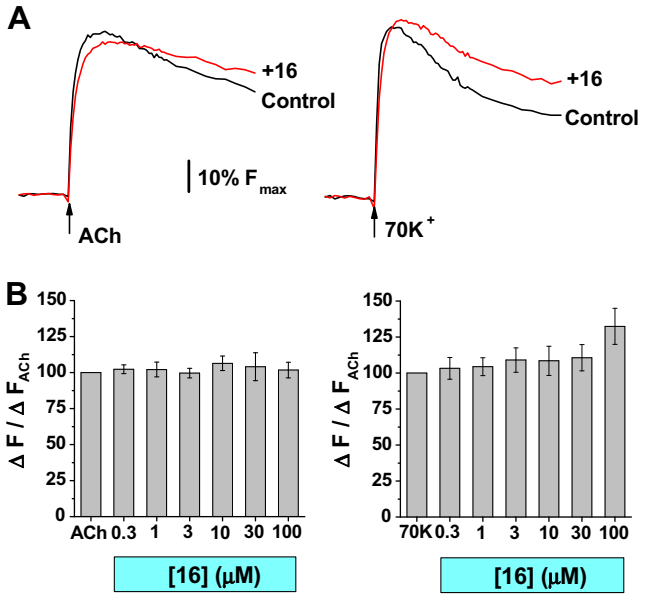

Figure 5. Effects of compound **16** on calcium signals in bovine chromaffin cell populations. Panel A shows representative recordings of the increase of $[Ca^{2+}]_c$ in bovine chromaffin cell populations stimulated with ACh or K^+. Data are expressed as% of F_{max}. Panel B shows averaged data obtained in 12 dishes (from four different cell cultures) upon application of ACh or K^+ in the absence or in the presence of increasing concentrations of compound **16**. Data have been normalized with respect to the initial response to ACh or K^+.

4. Experimental part

4.1. General methods

Melting points were determined on a Koffler apparatus, and are uncorrected. ^{1}H NMR and ^{13}C NMR spectra were recorded at rt in $CDCl_3$ or DMSO-d_6 at 300, 400 or 500 MHz and at 75, 100 or 125 MHz, respectively, using solvent peaks ($CDCl_3$: 7.27 (*D*), 77.2 (*C*) ppm; D_2O: 4.60 ppm and DMSO-d_6: 2.49 (D), 40 (C)) as internal reference. The assignment of chemical shifts is based on standard NMR experiments (^{1}H, ^{13}C-DEPT, ^{1}H, ^{1}H-COSY, gHSQC, gHMBC). Mass spectra were recorded on a GC/MS spectrometer with an API-ES ionization source. Elemental analyses were performed at CQO (CSIC, Spain). TLC was performed on silica F254 and detection by UV light at 254 nm or by charring with either ninhydrin, anisaldehyde or phosphomolybdic-H_2SO_4 dyeing reagents. Anhydrous solvents were used in all experiments. Column chromatography was performed on Silica Gel 60 (230 mesh). Reactions under MW irradiation (250 W) were performed in a CEM Discover system™, equipped with electromagnetic sample stirrer, an infrared temperature detector and a pressure sensor. The reaction was performed in 30 mL glass tube equipped with septa.

4.1.1. General procedure for the synthesis of 6,7,8,9-tetrahydrobenzo[1,8-*b*]-naphthyridin-5-amine derivatives III

Method A.[21a] In a 20 mL glass tube equipped with septa, precursors (1 equiv) were dissolved in distilled 1,2-dichloroethane. To this solutions $AlCl_3$ (1.5 equiv) and cyclohexanone (1.5 equiv) were added. The reaction mixture was stirred for 30 s, and then exposed to MW irradiation at 95 °C during the time indicated for each compound. When the reaction was over (TLC analysis: CH_2Cl_2/EtOAc, 10:1, v/v), the reaction mixture was diluted with a solution of THF/water (1:1); then, an aqueous solution of sodium hydroxide (10%) was added till pH 11–12. After stirring for 30 min, the mixture was extracted with CH_2Cl_2, dried over anhydrous sodium sulphate, filtered and the solvent evaporated. The resultant solid was purified by column chromatography using methanol/dichloromethane mixtures (1–15%) as eluent to give pure final products. *Method B.*[28] To solution of the precursor (1 equiv) and the appropriate 1-alkyl-4-piperidone (1.3 equiv) in dry ethyl acetate, TMSOTf was added dropwise. The reaction mixture was heated during the time indicated for each compound. After cooling, the precipitate was filtered, dissolved in a mixture of EtOH/H_2O (1:2) and basified with an aqueous solution of sodium hydroxide 1 M. After extraction with EtOAc, the organic layer was dried with anhydrous sodium sulfate and concentrated. The resulting crude was purified by column chromatography.

4.1.2. 5-Amino-2-(dimethylamino)-6,7,8,9-tetrahydrobenzo[1,8-*b*]-naphthyridine-3-carbonitrile (11)

Following the general procedure (Method A), reaction of compound **1**[21b] (200 mg, 1.1 mmol), cyclohexanone (166 μL, 1.6 mmol), and $AlCl_3$ (211 mg, 1.6 mmol) in $Cl(CH_2)_2Cl$ (11 mL), after 85 min of irradiation and column chromatography (1–15% of MeOH in dichloromethane), gave product **11** (207 mg, 72%): mp 250–252 °C; IR (KBr) ν 3474, 3299, 3217, 2939, 2850, 2207, 1627, 1599, 1540, 1519, 1394 cm^{-1}; ^{1}H NMR (300 MHz, $CDCl_3$) δ 8.34 (s, 1H), 4.91 (s, 2H), 3.33 (s, 6H), 2.96 (t, J = 5.6 Hz, 2H), 2.49 (t, J = 5.6 Hz, 2H), 1.87 (m, 4H); ^{13}C NMR (75 MHz, $CDCl_3$) δ 165.6, 158.5, 148.7, 142.0, 119.6, 109.9, 104.7, 92.8, 41.2 (2C), 34.9, 23.8, 23.1 (2C); MS (IE) *m/z* (%): 267 (M^+, 72), 252 (90), 238 (100). Anal. Calcd for $C_{15}H_{17}N_5$: C, 67.39; H, 6.41; N, 26.20. Found: C, 67.16; H, 6.70; N, 25.98.

4.1.3. 5-Amino-2-pyrrolidin-1-yl-6,7,8,9-tetrahydrobenzo[1,8-*b*]-naphthyridine-3-carbonitrile (12)

Following the general procedure (Method A), reaction of compound **2**[24] (200 mg, 0.94 mmol) with cyclohexanone (146 μL, 1.4 mmol) and $AlCl_3$ (186 mg, 1.4 mmol) in $Cl(CH_2)_2Cl$ (9.4 mL) after 4.5 h, and column chromatography (1% of MeOH in dichloromethane), gave product **12** (272 mg, 98%): mp 270–272 °C; IR (KBr) *ν* 3473, 3300, 3216, 2648, 2870, 2210, 1627, 1600, 1539, 1481, 1437, 1365, 1236 cm^{-1}; ^1H NMR (300 MHz, $CDCl_3$) *δ* 8.30 (s, 1H), 4.90 (s, 2H), 3.86 (dt, *J* = 6.6, 3.3 Hz, 4H), 2.95 (t, *J* = 5.7 Hz, 2H), 2.47 (t, *J* = 5.8 Hz, 2H), 2.02–1.93 (m, 4H), 1.86 (d, *J* = 5.7 Hz, 5H); ^{13}C NMR (75 MHz, $CDCl_3$) *δ* 164.8, 155.4, 155.0, 148.8, 141.9, 119.6, 108.8, 103.9, 91.3, 49.2 (2C), 34.4, 25.7 (2C), 23.3, 22.7 (2C); MS (IE) *m/z* (%): 293 (M^+, 57), 263 (76), 262 (100), 238 (67), 198 (17). Anal. Calcd for $C_{17}H_{19}N_5$: C, 69.60; H, 6.53; N, 23.87. Found: C, 69.55; H, 6.28; N, 23.76.

4.1.4. 5-Amino-2-piperidin-1-yl-6,7,8,9-tetrahydrobenzo[1,8-*b*]-naphthyridine-3-carbonitrile (13)

Following the general procedure (Method A), reaction of compound **3**[24] (250 mg, 1.1 mmol) with cyclohexanone (170 μL, 1.6 mmol) and $AlCl_3$ (217 mg, 1.6 mmol) in $Cl(CH_2)_2Cl$ (11 mL), after 3 h and 45 min, and column chromatography (1–5% of MeOH in dichloromethane), gave product **13** (310 mg, 91%): mp 240–242 °C; IR (KBr) *ν* 3471, 3307, 3221, 2929, 2852, 2831, 2216, 1630, 1600, 1542, 1433, 1347, 1281, 1253, 1238 cm^{-1}; ^1H NMR (300 MHz, $CDCl_3$) *δ* 8.62 (s, 1H), 5.54 (s, 2H), 3.68 (s, 4H), 2.98 (t, *J* = 5.4 Hz, 2H), 2.49 (t, *J* = 5.4 Hz, 2H), 1.86 (d, *J* = 5.1 Hz, 4H), 1.64 (s, 6H); ^{13}C NMR (75 MHz, $CDCl_3$) *δ* 163.3, 159.3, 154.2, 149.7, 142.1, 118.5, 109.8, 104.6, 94.7, 49.6 (2C), 33.6, 26.0 (2C), 24.6, 23.3, 22.5, 22.5; MS (IE) *m/z* (%): 307 (M^+, 99), 278 (100), 265 (41), 251 (38), 224 (44), 198 (38). Anal. Calcd for $C_{18}H_{21}N_5$: C, 70.33; H, 6.89; N, 22.78. Found: C, 70.15; H, 6.88; N, 22.59.

4.1.5. 5-Amino-2-(prop-2-yn-1-ylamino)-6,7,8,9-tetrahydrobenzo[1,8-*b*]-naphthyridine-3-carbonitrile (14)

Following the general procedure (Method A), reaction of compound **4**[21b] (197 mg, 1.0 mmol) with cyclohexanone (0.15 mL, 1.5 mmol) and $AlCl_3$ (198 mg, 1.5 mmol) in $Cl(CH_2)_2Cl$ (10 mL), after 3.5 h, and column chromatography (5% of MeOH and 0.5% of Et_3N in dichloromethane), gave product **14** (215 mg, 78%): mp >230 °C; IR (KBr) *ν* 3470, 3368, 3294, 3222, 2940, 2214, 1628, 1613, 1548, 1520 cm^{-1}; ^1H NMR (300 MHz, $CDCl_3$) *δ* 8.98 (s, 1H, CH), 7.67 (br s, 1H, NH), 6.48 (s, 4H), 2.98 (t, *J* = 5.4 Hz, 2H), 2.49 (t, *J* = 5.4 Hz, 2H), 1.86 (d, *J* = 5.1 Hz, 4H), 1.64 (s, 6H); ^{13}C NMR (75 MHz, $CDCl_3$) *δ* 161.4, 155.2, 154.3, 141.1, 141.2, 116.7, 108.5, 103.5, 90.8, 82.0, 72.2, 32.8, 30.0, 23.0, 22.0 (2C); MS (IE) *m/z* (%): 277 (M^+,100), 262 [$(M-CN)^+$, 15], 251 (21), 223 (38), 205 (25). Anal. Calcd for $C_{16}H_{15}N_5 \cdot HCl \cdot 3/2H_2O$: C, 56.39; H, 5.62; Cl, 10.40; N, 20.55. Found: C, 56.50; H, 5.37; Cl, 9.84; N, 20.29.

4.1.6. 5-Amino-2-(dimethylamino)-4-phenyl-6,7,8,9-tetrahydrobenzo[1,8-*b*]-naphthyridine-3-carbonitrile (15)

Following the general procedure (Method A), reaction of compound **5**[21b] (200 mg, 0.8 mmol), cyclohexanone (118 μL, 1.1 mmol) and $AlCl_3$ (150 mg, 1.1 mmol) in $Cl(CH_2)_2Cl$ (6 mL) after 2 h, and column chromatography (10% of EtOAc and 1% of Et_3N in dichlormethane), gave compound **15** (124 mg, 47%): mp 222–224 °C; IR (KBr) 3484, 2928, 2210, 1625, 1557, 1390 cm^{-1}; ^1H NMR (300 MHz, $CDCl_3$) *δ* 7.74–7.46 (m, 3H), 7.49–7.29 (m, 2H), 4.28 (s, 2H), 3.32 (s, 6H), 2.98 (t, *J* = 5.1 Hz, 2H), 2.26 (t, *J* = 5.8 Hz, 2H), 1.83 (d, *J* = 6.5 Hz, 4H); ^{13}C NMR (75 MHz, $CDCl_3$) *δ* 163.4, 158.3, 157.2, 154.6, 149.5, 136.8, 129.9, 129.4 (2C), 128.0 (2C), 116.9, 109.3, 102.8, 94.8, 40.7 (2C), 33.7, 23.0, 22.3, 22.1; MS (API-ES+): 344 [$(M+H)^+$]. Anal. Calcd for $C_{21}H_{21}N_5$: C, 73.44; H, 6.16; N, 20.39. Found: C, 73.17; H, 6.42; N, 20.10.

4.1.7. 5-Amino-2-(methyloxy)-6,7,8,9-tetrahydrobenzo[1,8-*b*]-naphthyridine-3-carbonitrile (16)

Following the general procedure (Method A), reaction of compound **6**[25] (87 mg, 0.5 mmol) with cyclohexanone (57 μL, 0.6 mmol) and $AlCl_3$ (113.3 mg, 0.8 mmol) in $Cl(CH_2)_2Cl$ (5 mL), after 32 min, and column chromatography (5% of MeOH in dichloromethane) gave product **16** (87 mg, 95%); mp 259–260 °C; IR (KBr) *ν* 3351, 3181, 3058, 2229, 1661, 1594, 1540, 1397, 1271, 1223 cm^{-1}; ^1H NMR (400 MHz, DMSO-d_6) *δ* 9.36 (s, 1H, H4), 7.23 (m, 2H, NH_2), 2.84 (m, 2H, CH_2, H6), 1.80 (m, 2H, CH_2, H9), 1.22 (m, 4H, $2CH_2$, H7 and H8); ^{13}C NMR (100 MHz, DMSO-d_6) *δ* 163.1, 160.8, 154.0, 150.6, 142.1, 116.0, 109.9, 105.9, 91.9, 54.1, 33.7, 23.2, 22.1, 22.0; MS (API-ES+): 255 [$(M+H)^+$], Anal. Calcd for $C_{14}H_{14}N_4O$: C, 66.13; H, 5.55; N, 22.03. Found: C, 66.07; H, 5.72; N, 21.98. The free base was dissolved in dry ethyl ether, and HCl/ethyl ether was added dropwise with stirring. A white precipitate was formed immediately. The precipitate was separated by filtration, washed with ether and dried in vacuo to afford a white powder: mp 265–268 °C; IR (KBr) *ν* 3060, 2944, 2234, 1661, 1629, 1602, 1477, 1408, 1305 cm^{-1}; Anal. Calcd for $C_{14}H_{15}ClN_4O$: C, 57.83; H, 5.20; N, 19.27. Found: C, 57.58; H, 5.48; N, 19.42.

4.1.8. 5-Amino-2-(ethyloxy)-6,7,8,9-tetrahydrobenzo[1,8-*b*]-naphthyridine-3-carbonitrile (17)

Following the general procedure (Method A), reaction of compound **7**[26] (200 mg, 1.1 mmol) with cyclohexanone (165 μL, 1.6 mmol) and $AlCl_3$ (213 mg, 1.6 mmol) in $Cl(CH_2)_2Cl$ (10 mL), after 30 min, and column chromatography (5% of MeOH in dichloromethane), gave product **17** (260 mg, 92%): mp 265–267 °C; IR (KBr) *ν* 3333, 3232, 2929, 2851, 2222, 1636, 1614, 1455, 1296 cm^{-1}; ^1H NMR (300 MHz, DMSO-d_6) *δ* 9.16 (s, 1H, CH), 6.94 (br s, 2H, NH_2), 4.48 (q, *J* = 7.1 Hz, 2H, CH_2), 2.79 (m, 2H, CH_2), 2.46 (t, *J* = 6.0 Hz, 2H, CH_2), 1.80 (m, 4H, 2 x CH_2), 1.38 (t, *J* = 7.1 Hz, 3H, CH_3). ^{13}C NMR (75 MHz, DMSO-d_6) *δ* 163.0, 160.5, 154.0, 150.6, 142.1, 116.0, 109.9, 105.8, 92.0, 62.5, 33.6, 23.2, 22.1, 22.0, 14.2; MS (IE) *m/z* (%): 268 (M^+, 59), 253 (89), 240 (100), 223 (36). Anal. Calcd for $C_{15}H_{16}N_4O$: C, 67.15; H, 6.01; N, 20.88. Found: C, 67.03; H, 6.28; N, 21.04.

4.1.9. 5-Amino-2-methoxy-4-phenyl-6,7,8,9-tetrahydrobenzo[1,8-*b*]-naphthyridine-3-carbonitrile (18)

Following the general procedure (Method A), reaction of compound **8**[27] (300 mg, 1.2 mmol) with cyclohexanone (180 μL, 1.8 mmol) and $AlCl_3$ (237 mg, 1.8 mmol) in $Cl(CH_2)_2Cl$ (12 mL), after 12 h, and column chromatography (1–5% of MeOH in dichloromethane), gave product **18** (266 mg, 67%); mp 300–302 °C; IR (KBr) *ν* 3515, 3419, 3392, 3036, 2937, 2862, 2223, 1591, 1574, 1547, 1504, 1431, 1379, 1314, 1269, 1161 cm^{-1}; ^1H NMR (300 MHz, $CDCl_3$) *δ* 7.74–7.52 (m, 3H), 7.54–.33 (m, 2H), 4.41 (br s, 2H, NH_2), 4.21 (s, 3H, CH_3), 3.04 (t, *J* = 5.5 Hz, 2H), 2.31 (t, *J* = 5.3 Hz, 2H), 1.88 (d, *J* = 2.7 Hz, 4H). ^{13}C NMR (75 MHz, $CDCl_3$) *δ* 163.9, 161.6, 156.8, 155.1, 150.0, 136.5, 130.6, 129.6 (2C), 128.0 (2C), 115.0, 111.5, 104.6, 97.2, 55.1, 34.4, 23.4, 22.6, 22.5; MS (API-ES+): 331 [$(M+H)^+$, 100], 353 [$(M+Na)^+$, 18]. Anal. Cald. for $C_{20}H_{18}N_4O$: C, 72.71; H, 5.49; N, 16.96. Found: C, 72.58; H, 5.20; N, 16.70.

4.1.10. 5-Amino-2-chloro-6,7,8,9-tetrahydrobenzo[1,8-*b*]-naphthyridine-3-carbonitrile (19)

Following the general procedure (Method A), reaction of compound **9**[21b] (200 mg, 1.1 mmol) with cyclohexanone (174 μL, 1.7 mmol) and $AlCl_3$ (221 mg, 1.7 mmol) in $Cl(CH_2)_2Cl$ (11.2 mL), after 4.5 h of irradiation, and column chromatography (1–5% of MeOH in dichloromethane), gave product **19** (88 mg, 30%): mp >270 °C; IR (KBr) *ν* 3351, 3181, 3058, 2229, 1661, 1594, 1540, 1397, 1271, 1223 cm^{-1}; ^1H NMR (300 MHz, DMSO-d_6) *δ* 9.36 (s,

1H, H4), 7.23 (br s, 2H, NH_2), 2.84 (m, 2H, H6), 1.80 (m, 2H, H9), 1.22 (m, 4H, H7 and H8); ^{13}C NMR (75 MHz, DMSO-d_6) δ 165.4, 154.6, 151.4, 149.5, 143.0, 116.6, 112.6, 109.6, 102.6, 27.9, 22.7, 20.6, 20.1; MS (API-ES+): 259 [$(M+H)^+$, 100] 281 [$(M+Na)^+$], 353. Anal. Calcd for $C_{13}H_{11}ClN_4$: C, 60.35; H, 4.29; N, 21.66; Cl, 13.70. Found: C, 60.18; H, 4.49; N, 21.37; Cl, 13.49.

4.1.11. 5-Amino-2-chloro-4-phenyl-6,7,8,9-tetrahydrobenzo[1,8-*b*]-naphthyridine-3-carbonitrile (20)

Following the General procedure (Method A), reaction of compound **10**[21b] (100 mg, 0.4 mmol) with cyclohexanone (174 μL, 1.7 mmol) and $AlCl_3$ (78 mg, 0.6 mmol) in $Cl(CH_2)_2Cl$ (5 mL), after 60 h, and column chromatography (from 1% to 4% of MeOH in dichloromethane), afforded product **20** (30 mg, 20%): mp >270 °C; IR (KBr) ν 3498, 3334, 3230, 2931, 1725, 1629, 1571, 1540, 1445, 1269, 1223 cm^{-1}; ^{1}H NMR (300 MHz, DMSO-d_6) δ 7.68 (d, 2H, 2CH, 2′,6′-Py), 7.59 (d, 2H, 2CH, 3′,5′-Py), 5.50 (s, 2H, NH_2), 2.85 (m, 2H, CH_2, H6), 2.31 (m, 2H, CH_2, H9), 1.78 (m, 4H, $2CH_2$, H7, H8); ^{13}C NMR (75 MHz, DMSO-d_6) 158.1, 156.5, 154.5, 153.9, 147.5, 133.5, 131.6, 130.5 (2C), 127.9 (2C), 113.8, 113.6, 109.6, 106.6, 27.9, 22.7, 20.6, 20.1; MS (API-ES+): 335.2 [$(M+1)^+$, 100], 357.2 [$(M+Na)^+$]. Anal. Calcd for $C_{19}H_{15}N_4Cl$: C, 68.16; H, 4.52; N, 16.73. Found: C, 67.98; H, 4.70; N, 16.91.

4.1.12. 5-Amino-7-benzyl-2-methoxy-6,7,8,9-tetrahydropyrido[2,3-*b*][1,6]naphthyridine-3-carbonitrile (21)

Following the general procedure (Method B),[28] reaction of compound **6**[25] (200 mg, 1.2 mmol) with 1-benzyl-4-piperidone (0.26 mL, 1.5 mmol) and TMSOTf (0.48 mL, 2.6 mmol) in dry EtOAc (2.4 mL) after 20 h, and recrystallization from EtOH, gave pure product **21** (320 mg, 81%): mp 210–212 °C; IR (KBr) ν 3462, 3375, 2225, 1618, 1552, 1351, 1293 cm^{-1}; ^{1}H NMR (300 MHz, $CDCl_3$) δ 8.45 (s, 1H), 7.42–7.25 (m, 5H), 4.84 (s, 2H), 4.16 (s, 3H), 3.78 (s, 2H), 3.48 (s, 2H), 3.15 (t, J = 5.8 Hz, 2H), 2.87 (t, J = 5.8 Hz, 2H); ^{13}C NMR (75 MHz, $CDCl_3$) δ 162.8, 155.4, 147.7, 140.2, 138.3, 129.6 (2C), 129.1 (2C), 128.1, 116.2, 110.1, 106.6, 95.6, 63.4, 55.6, 51.3, 50.3, 34.6; MS (IE) m/z (%): 345 (M^+, 55), 344 (100), 328 (30), 254 (49), 91 (44). Anal. Calcd for $C_{20}H_{19}N_5O$: C, 69.55; H, 5.54; N, 20.28. Found: C, 69.51; H, 5.36; N, 20.02.

4.1.13. 5-Amino-7-benzyl-2-chloro-6,7,8,9-tetrahydropyrido[2,3-*b*][1,6]naphthyridin-3-carbonitrile (22)

Following the general procedure (Method B),[28] reaction of compound **9**[21b] (200 mg, 1.1 mmol) with 1-benzyl-4-piperidone (0.26 mL, 1.4 mmol) and TMSOTf (0.47 mL, 2.6 mmol) in dry EtOAc (2.3 mL) after 48 h, and purification by column chromatography (5% MeOH and 0.5% Et_3N in dichloromethane), gave the product **22** (211 mg, 54%): mp >300 °C; IR (KBr) ν 3345, 3244, 2845, 2756, 2232, 1629, 1592, 1541, 1347, 1273 cm^{-1}; ^{1}H NMR (300 MHz, DMSO-d_6) δ 9.39 (s, 1H), 7.54–7.16 (m, 5H), 3.75 (s, 2H), 3.49 (s, 2H), 2.93 (t, J = 5.7 Hz, 2H), 2.75 (t, J = 5.7 Hz, 2H); ^{13}C NMR (75 MHz, DMSO-d_6) δ 162.5, 154.3, 149.2, 149.1, 142.4, 137.9, 128.8 (2C), 128.2, 127.0, 115.9, 110.3, 109.3, 102.20, 61.4, 51.0, 48.7, 33.5; MS (IE) m/z (%): 350 (M^+, 20), 348 (45), 258 (48), 91 (100). Anal. Calcd for $C_{19}H_{16}ClN_5$: C, 65.24; H, 4.61; N, 20.02; Cl, 10.13. Found: C, 64.99; H, 4.37; N, 19.93; Cl, 10.18.

4.2. Pharmacology

4.2.1. Inhibition experiments of AChE and BuChE

To assess the inhibitory activity of the compounds towards AChE or BuChE, we followed the spectrophotometric method of Ellman,[29] using purified AChE from *Electrophorus electricus* (Type V-S), bovine erythrocytes (Type XII-S) or BuChE from horse serum (lyophilized powder) (Sigma Aldrich, Madrid, Spain). The reaction took place in a final volume of 3 mL of a phosphate-buffered solution (0.1 M) at pH 8, containing 0.035 U of AChE or 0.05 U of BuChE, and 0.35 mM of 5,5′-dithiobis-2-nitrobenzoic acid (DTNB, Sigma Aldrich, Madrid, Spain). Inhibition curves were made by pre-incubating this mixture with at least nine concentrations of each compound for 10 min. A sample with no compound was always present to determine the 100% of enzyme activity. After this pre-incubation period, acetylthiocholine iodide (ATChI, 0.35 mM) or butyrylthiocholine iodide (BuTChI, 0.5 mM) (Sigma Aldrich, Madrid, Spain) were added, allowing 15 min more of incubation, where the DTNB produces the yellow anion 5-thio-2-nitrobenzoic acid along with the enzymatic degradation of ATChI or BuTChI. Changes in absorbance were detected at 405 nm in a spectrophotometric plate reader (FluoStar OPTIMA, BMG Labtech). Compounds inhibiting AChE or BuChE activity would reduce the color generation, thus IC_{50} values were calculated as the concentration of compound that produces 50% AChE activity inhibition. Data are expressed as means ± SEM of at least three different experiments in quadruplicate.

4.2.2. Kinetic analysis of the AChE inhibition

To obtain estimates of the competitive inhibition constant K_i, reciprocal plots of $1/V$ versus $1/[S]$ were constructed at different concentrations of the substrate acetylthiocholine (0.1–1 mM) by using Ellman's method.[29] Experiments were performed in a transparent 48-well plate, with a final volume of 1 mL, containing each well DTNB 0.35 mM, 1 μL DMSO (control) or inhibitor solution to give desired final concentration. Reaction was initiated by adding 45 μL of AChE (final concentration 0.18 U/mL) at 30 °C to give a final. Progress curves were monitored at 412 nm for 2 min in a fluorescence plate reader Fluostar Optima (BMG-technologies, Germany) absorbance ready. Progress curves were characterized by a linear steady-state turnover of the substrate and values of a linear regression were fitted according to Lineweaver–Burk replots using Origin software. The plots were assessed by a weighted least square analysis. Determination of Michaelis constant for the substrate ATCh was done at five different concentrations (0.1–1 mM) to give a value of K_M = 0.27 ± 0.02 mM, and V_{max} = 1.0 ± 0.1 min^{-1}. Slopes of the reciprocal plots were then plotted against the concentration of **16** (range 0–0.3 μM) as described,[42] to evaluate K_i data. Data analysis was performed with Origin Pro 7.5 software (Origin Lab Corp.).

4.2.3. Molecular modelling of inhibitor 16

The X-ray crystal structure of *Torpedo californica* acetylcholinesterase (PDB code 1ACJ)[43] at 2.80 Å resolution was retrieved from the Protein Data Bank (http://www.rcsb.org/pdb/). Charges were assigned to ligand atoms (compound **16**) with MOPAC (MOPAC)[44] ESP with MNDO method.[45] The Lamarckian genetic algorithm implemented in AUTODOCK 4.0[46] (http://autodock.scripps.edu/) was used to generate docked conformations of inhibitor **16** within the binding site by randomly changing the overall orientation of the molecule as well as the torsion angles of all routable bonds. A volume of exploration was defined in the shape of a three-dimensional cubic grid ($40 \times 40 \times 40$ Å^3) with a spacing of 0.375 Å. At each grid point, the enzyme's atomic affinity potentials for carbon, aromatic carbon, oxygen, nitrogen and hydrogen atoms were recalculated for rapid intra- and intermolecular energy evaluation of the docking solutions **16**.

4.2.4. Molecular dynamics simulations (MD)

The MD simulations were carried out using the AMBER 10 suite of programs.[47] The bonded and no bonded parameters were assigned from those already present in the AMBER database in a way consisted with the second-generation force field (parm 99).[48] The molecular system was neutralized by the addition of three chlorine ions,[49] and immersed in a truncated octahedron of ~3760 TIP3P water

molecules.[50] Periodic boundary conditions were treated using the smooth particle mesh Ewald method[51] with a grid spacing of 1 Å. The cutoff distance for the non-bonded interactions was 9 Å. The SHAKE algorithm[52] was applied to all bonds and an integration step of 2.0 fs was used throughout. Solvent molecules and counter ions were relaxed by energy minimization and allowed to redistribute around the positionally restrained solute (25 kcal mol^{-1} $Å^2$) during 50 ps of MD at constant temperature (300 K) and pressure (1 atm). These initial harmonic restraints were gradually decreased in a series of progressive energy minimizations until they were completely removed. The resulting system was heated again from 100 to 300 K during 20 ps and allowed to equilibrate in the absence of any restraints for 2 ns during which system coordinates were collected every 2 ps for further analysis. The resulting trajectories and structures were visually inspected using the computer graphics program PYMOL[53] and analyzed with the PTRAJ module of AMBER 10.

4.2.5. MM-GBSA binding calculations

Effective binding free energy was qualitatively estimated using the MM-GBSA approach.[54] MM-GBSA method approaches free energy of binding as a sum of molecular mechanics (MM) interaction term, a salvations contribution thorough a generalized Born (GB) model, and a surface area (SA) contribution to account for the non polar part of desolvation. These calculations were performed for each snapshot from the simulation using the appropriate module within AMBER 10 and averaged out.

4.2.6. Quantification of viability by the MTT reduction method in SH-SY5Y cells

Cell viability, virtually the mitochondrial activity of living cells, was measured by quantitative colorimetric assay with MTT (3-[4,5-dimethylthiazol-2-yl]-2,5-diphenyl-tetrazolium bromide, Sigma Aldrich, Madrid, Spain), as described previously.[55] SH SY5Y cells were seeded into 48-well culture plates and allowed to attach. MTT was added to all wells (5 mg/mL) and allowed to incubate, in the dark at 37 °C for 2 h followed by cell lysis and spectrophotometrically measurement at 540 nm. The tetrazolium ring of MTT can be cleaved by active reductases in order to produce a precipitated formazan derivative. The formazan produced was dissolved by adding 300 μL DMSO, resulting in a colored compound whose optical density was measured in an ELISA reader at 540 nm. All MTT assays were performed in triplicate.

4.2.7. Measurement of lactate dehydrogenase activity

Samples of incubation media were collected at the end of a 24 h period of exposure to the toxic to estimate extracellular LDH, an indication of cell death.[56] LDH activity was also measured in the cells after treatment with 10% Triton X-100 (intracellular LDH). LDH activity was measured spectrophotometrically at 490–620 nm, using a microplate reader (Labsystems iEMS reader MF; Labsystems, Helsinki, Finland). Total LDH (intracellular plus extracellular) was normalized to 100%; then, the amount of LDH released to the extracellular medium was expressed as percentage of this total. Data were normalized by subtracting basal LDH (cells not subjected to any treatment) to the different treatment groups in each individual experiment, and the result for rot/oligo group was normalized to 100% (percentage cell death).

4.2.8. Neuroprotection experiments with okadaic acid

To evaluate neuroprotection against okadaic acid 30 nM which reproduce the characteristic pathology of AD (neurofibrillary tangles of τ-protein,[39,40] the following protocol was used: SH-SY5Y cells were exposed for 24 h to 30 nM okadaic acid; Compound **16** was administered at the concentrations of 0.1–3 μM, 24 h before cell incubation with the toxic stimuli and maintained during an additional 24-h period. At the end of the experiments, cell death was assessed by measuring the activity of lactate dehydrogenase (LDH) released.

4.2.9. Neuroprotection experiments with rotenone/oligomycin-A

The neuroprotective effect of the compounds against this toxic stimulus was evaluated with the method of MTT reduction, at the concentration of 1 μM on SH-SY5Y neuroblastoma cells, exposed to 30 μM rotenone plus 10 μM oligomycin-A for 24 h.

4.2.10. Isolation and culture of bovine chromaffin cells

Bovine chromaffin cells were isolated from adrenal glands of adult cows, following standard methods[57] with some modifications.[58] Cells were suspended in Dulbeccós modified Eaglés medium (DMEM) supplemented with 5% foetal calf serum, 10 μM cytosine arabinoside, 10 μM fluorodeoxyuridine, 50 IU ml^{-1} penicillin and 50 μg/ml streptomycin. Cells were plated at a density of 2×10^5 cells per well into 96-well plates. Cells were kept for 2 days at 37 °C in a water-saturated incubator, with a 5% CO_2/95% air atmosphere. Experiments were performed at room temperature (24 ± 2 °C).

4.2.11. Measurement of $[Ca^{2+}]_c$ in bovine chromaffin cells

Cells were loaded with Krebs-HEPES (in mM: 144 NaCl, 5.9 KCl, 1.2 $MgCl_2$, 2 $CaCl_2$, 11 D-glucose, 10 HEPES, pH 7.4) containing 10 μM fluo-4 AM, and 0.2% pluronic acid for 45 min at 37 °C in the dark. After this incubation period, cells were washed twice with Krebs-HEPES at room temperature in the dark. Changes in fluorescence (excitation 485 nm, emission 520 nm) were measured using a fluorescent plate reader (Fluostar, BMG Labtechnologies). Basal levels of fluorescence were monitored before adding stimulation solutions (100 μM ACh or 70 mM K^+) by using an automatic dispenser. After stimulation, changes in fluorescence were measured for 40 seg. To normalize fluo-4 signals, responses from each well were calibrated by measuring maximum and minimum fluorescence values. At the end of each experiment, addition of 3% Triton X-100 (F_{max}) was followed by addition of 1 M $MnCl_2$ (F_{min}). Data were calculated as a percentage of $F_{max} - F_{min}$.

Acknowledgments

A. Samadi thanks CSIC for a I3P-post-doc contract. M. Chioua thanks Instituto de Salud Carlos III (MICINN) for a 'Sara Borrell' post-doctoral contract. J.M.C. thanks MICINN (SAF2006-08764-C02-01, SAF2009-07271), ISCIII [Red RENEVAS (RD06/0026/0009, RD06/0026/1002)]), CAM (S/SAL-0275-2006), and CSIC-GRICES (2007PT-13) financial support. The present work has also been supported by Fundación Teófilo Hernando, MEC Grants BFI2003-02722, SAF-2006-08540, SAF2006-1249 and CTQ2005-09365, and Fundación La Caixa (Barcelona, Spain). L.G. thanks MICINN for support (SAF 2007-65181). M.G.L. thanks MICINN for support (SAF 2009-12150). M.V. thanks Fundación CIEN for support (Instituto de Salud Carlos III). Ágatha Bastida thanks Eva Priego (IQM, CSIC) for the molecular dynamic analysis of compound **16**.

References and notes

1. Goedert, M.; Spillantini, M. G. A. *Science* **2006**, *314*, 777.
2. Castro, A.; Martínez, A. *Curr. Pharm. Des.* **2006**, *12*, 4377.
3. Cummings, J. L. *Rev. Neurol. Dis.* **2004**, *1*, 60.
4. Scarpini, E.; Scheltens, P.; Feldman, H. *Lancet Neurol.* **2003**, *2*, 539.
5. Talesa, V. N. *Mech. Ageing Dev.* **2001**, *122*, 1961.
6. Racchi, M.; Mazzucchelli, M.; Porrello, E.; Lanni, C.; Govoni, S. *Pharmacol. Res.* **2004**, *50*, 441.
7. Inestrosa, N. C.; Álvarez, A.; Pérez, C. A.; Moreno, R. D.; Vicente, M.; Linker, C.; Casanueva, O. I.; Soto, C.; Garrido, J. *Neuron* **1996**, *16*, 881.

8. Bartolini, M.; Bertucci, C.; Cavrini, V.; Andrisano, V. *Biochem. Pharmacol.* **2003**, *65*, 407.
9. Cavalli, A.; Bolognesi, M. L.; Capsoni, S.; Andrisano, V.; Bartolini, M.; Margotti, E.; Cattaneo, A.; Recanatini, M.; Melchiorre, C. *Angew. Chem., Int. Ed.* **2007**, *46*, 3689.
10. Muñoz-Torrero, D.; Camps, P. *Curr. Med. Chem.* **2006**, *13*, 399.
11. Savini, L.; Gaeta, A.; Fattorusso, C.; Catalanotti, B.; Campiani, G.; Chiasserini, L.; Pellerano, C.; Novellino, E.; McKissic, D.; Saxena, A. *J. Med. Chem.* **2003**, *46*, 1.
12. Decker, M. *J. Med. Chem.* **2006**, *49*, 5411.
13. Carlier, P. R.; Chow, E. S.; Han, Y.; Liu, J.; El Yazal, J.; Pang, Y. P. *J. Med. Chem.* **1999**, *42*, 4225.
14. Cavalli, A.; Bolognesi, M. L.; Minarini, A.; Rosini, M.; Tumiatti, V.; Recanatini, M.; Melchiorre, C. *J. Med. Chem.* **2008**, *51*, 347.
15. Rodríguez-Franco, M. I.; Fernández-Bachiller, M. I.; Pérez, C.; Hernández-Ledesma, B.; Bartolomé, B. *J. Med. Chem.* **2006**, *49*, 459.
16. Sterling, J.; Herzig, Y.; Goren, T.; Finkelstein, N.; Lerner, D.; Goldenberg, W.; Miskolczi, I.; Molnar, S.; Rantal, F.; Tamas, T.; Toth, G.; Zagyva, A.; Zekany, A.; Finberg, J.; Lavian, G.; Gross, A.; Friedman, R.; Razin, M.; Huang, W.; Krais, B.; Chorev, M.; Youdim, M. B.; Weinstock, M. *J. Med. Chem.* **2002**, *45*, 5260.
17. Toda, N.; Tago, K.; Marumoto, S.; Takami, K.; Ori, M.; Yamada, N.; Koyama, K.; Naruto, S.; Abe, K.; Yamazaki, R.; Hara, T.; Aoyagi, A.; Abe, Y.; Kaneko, T.; Kogen, H. *Bioorg. Med. Chem.* **2003**, *11*, 4389.
18. Rosini, M.; Antonello, A.; Cavalli, A.; Bolognesi, M. L.; Minarini, A.; Marucci, G.; Poggesi, E.; Leonardi, A.; Melchiorre, C. *J. Med. Chem.* **2003**, *46*, 4895.
19. Elsinghorst, P. W.; Cieslik, J. S.; Mohr, K.; Tränkle, C.; Gütschow, M. *J. Med. Chem.* **2007**, *50*, 5685.
20. (a) de los Ríos, C.; Egea, J.; Marco-Contelles, J.; León, R.; Samadi, A.; Iriepa, I.; Moraleda, I.; Gálvez, E.; García, A. G.; López, M. G.; Villarroya, M.; Romero, A. *J. Med. Chem.* **2010**, *53*, 5129; (b) Soriano, E.; Samadi, A.; Chioua, M.; de los Ríos, C.; Marco-Contelles, J. *Bioorg. Med. Chem. Lett.* **2010**, *20*, 2950.
21. (a) Marco-Contelles, J.; León, R.; de Los Ríos, C.; Samadi, A.; Bartolini, M.; Andrisano, V.; Huerttas, O.; Barril, X.; Luque, F. J.; Rodríguez-Franco, M. I.; López, B.; López, M. G.; García, A. G.; Carreiras, M. C.; Villarroya, M. *J. Med. Chem.* **2009**, *52*, 2724; (b) Samadi, A.; Marco-Contelles, J.; Soriano, E.; Álvarez-Pérez, M.; Chioua, M.; Romero, A.; González-Lafuente, L.; Gandía, L.; Roda, J. M.; López, M. G.; Villarroya, M.; García, A. G.; de los Ríos, C. *Bioorg. Med. Chem.* **2010**, *18*, 5861.
22. (a) Marco-Contelles, J.; Pérez-Mayoral, M. E.; Samadi, A.; Carreiras, M. C.; Soriano, E. *Chem. Rev.* **2009**, *109*, 2652; (b) Marco, José L.; Carreiras, Maria do Carmo *The Friedländer Reaction*; LAP Lambert Academic Publishing AG & Co.: KG, Saarbrücken (Germany), 2010.
23. Thomae, D.; Kirsch, G.; Seck, P. *Synthesis* **2008**, 1600.
24. Cocco, M. T.; Congiu, C.; Maccioni, A.; Onnis, V. *J. Heterocycl. Chem.* **1993**, *30*, 253.
25. (a) Harada, H.; Watanuki, S.; Takuwa, T.; Kawaguchi, K.; Okazaki, T.; Hirano, Y.; Saitoh, C. WO 2002006237.; (b) Fuentes, L.; Lorenzo, M. J.; Márquez, C.; Galakhov, M. *J. Heterocycl. Chem.* **1999**, *36*, 481; (c) Krapcho, A. P.; Huyffer, P. S. *J. Org. Chem.* **1963**, *28*, 2461; (d) Cottis, S. G.; Tieckelmann, H. *J. Org. Chem.* **1961**, *26*, 79.
26. Quintela, J. M.; Soto, J. L. *Anal. Quim.* **1984**, *80*, 268.
27. Álvarez-Insúa, A. S.; Lora-Tamayo, M.; Soto, J. L. *J. Heterocycl. Chem.* **1970**, *7*, 1305.
28. Sato, Y.; Tuda, M.; Nagai, M.; Yamazaki, H. WO 2000035918.
29. Ellman, G. L.; Courtney, K. D.; Andres, V., Jr.; Feather-Stone, R. M. *Biochem. Pharmacol.* **1961**, *7*, 88.
30. Bourne, Y.; Grassi, J.; Bougis, P. E.; Marchot, P. *J. Biol. Chem.* **1999**, *274*, 30370.
31. Ott, P.; Lustig, A.; Brodbeck, U.; Rosenbusch, J. P. *FEBS Lett.* **1982**, *138*, 187.
32. Liao, J.; Heider, H.; Sun, M. C.; Brodbeck, U. *J. Neurochem.* **1992**, *58*, 1230.
33. (a) Atack, J. R.; Yu, Q. S.; Soncrant, T. T.; Brossi, A.; Rapoport, S. I. *J. Pharmacol. Exp. Ther.* **1989**, *249*, 194; (b) Andersen, R. A.; Aaraas, I.; Gaare, G.; Fonnum, F. *Gen. Pharmacol.* **1977**, *8*, 331.
34. Chan, S. L.; Shirachi, D. Y.; Bhargava, H. N.; Gardner, E.; Trevor, A. J. *J. Neurochem.* **1972**, *19*, 2747.
35. Rampa, A.; Bisi, A.; Belluti, F.; Gobbi, S.; Valenti, P.; Andrisano, V.; Cavrini, V.; Cavalli, A.; Recanatini, M. *Bioorg. Med. Chem.* **2000**, *8*, 497.
36. Goodsell, D. S.; Morris, G. M.; Olson, A. J. *J. Mol. Recognit.* **1996**, *9*, 1.
37. Egea, J.; Rosa, A. O.; Cuadrado, A.; García, A. G.; López, M. G. *J. Neurochem.* **2007**, *102*, 1842.
38. Dodd, S.; Dean, O.; Copolov, D. L.; Malhi, G. S.; Berk, M. *Expert Opin. Biol. Ther.* **2008**, *8*, 1955.
39. (a) Pérez, M.; Hernández, F.; Gómez-Ramos, A.; Smith, M.; Perry, G.; Ávila, J. *Eur. J. Biochem.* **2002**, *269*, 1484; (b) Tian, Q.; Lin, Z. Q.; Wang, X. C.; Chen, J.; Wang, Q.; Gong, C. X.; Wang, J. Z. *Neuroscience* **2004**, *126*, 277.
40. Uberti, D.; Rizzini, C.; Spano, P. F.; Memo, M. *Neurosci. Lett.* **1997**, *235*, 149.
41. (a) Tanaka, T.; Zhong, J.; Iqbal, K.; Trenkner, E.; Grundke-Iqbal, I. *FEBS Lett.* **1998**, *426*, 248; (b) Arias, E.; Gallego-Sandín, S.; Villarroya, M.; García, A. G.; López, M. G. *J. Pharmacol. Exp. Ther.* **2005**, *315*, 1346.
42. Segel, I. H. *Enzyme Kinetics*; John Wiley: Toronto, Canada, 1975.
43. Harel, M.; Schalk, I.; Ehret-Sabtier, L.; Bouet, F.; Goeldner, M.; Hirth, C.; Axelsen, P. H.; Silman, I.; Sussman, J. L. *Proc. Natl. Acad. Sci. U.S.A.* **1993**, *90*, 9031.
44. Stewart, J. J. *J. Comput. Aided Mol. Des.* **1990**, *4*, 1.
45. Deward, M. J. S.; Thiel, W. *J. Am. Chem. Soc.* **1977**, *99*, 2338.
46. http://autodock.scripps.edu/.
47. Case, D. A.; Darden, T. A.; Cheatham, T. E., III; Simmerling, C. L.; Wang, J.; Duke, R. E.; Luo, R.; Walker, R. C.; Zhang, W.; Merz, K. M.; Roberts, B. P.; Wang, B.; Hayik, S.; Roitberg, A.; Seabra, G.; Kolossváry, I.; Wong, K. F.; Paesani, F.; Vanicek, J.; Wu, X.; Brozell, S.; Steinbrecher, R. T.; Gohlke, H.; Cai, Q.; Ye, X.; Wang, J.; Hsieh, M.-J.; Cui, G.; Roe, D. R.; Mathews, D. H.; Seetin, M. G.; Sagui, C.; Babin, V.; Luchko, T.; Gusarov, S.; Kovalenko, A.; Kollman, P. A. In *AMBER*; University of California: San Francisco, 2008; Vol. 10,
48. Cornell, W. D.; Cieplak, P.; Bayly, C. I.; Gould, I. R.; Merz, K. M.; Ferguson, D. M.; Spellmeyer, D. C.; Fox, T.; Caldwell, J. W.; Kollman, P. A. *J. Am. Chem. Soc.* **1995**, *117*, 5179.
49. Aqvist, J. *J. Phys. Chem.* **1990**, *94*, 8021.
50. Jorgensen, W. L.; Chandrasekhar, J.; Madura, J. D. *J. Chem. Phys.* **1983**, *79*, 926.
51. Darden, T. A.; York, D.; Pedersen, L. G. *J. Chem. Phys.* **1993**, *98*, 10089.
52. Ryckaert, J. P.; Ciccotti, G.; Berendsen, H. J. C. *J. Comput. Phys.* **1977**, *23*, 327.
53. DeLano, W. P. V. DeLano Scientific LLC, South San Francisco, CA, USA: http://www.pymol.org.
54. Still, W.; Tempezyk, A.; Hawley, R.; Hendrickson, T. *J. Am. Chem. Soc.* **1990**, *112*, 6127.
55. Denizot, F.; Lang, R. *J. Immunol. Methods* **1986**, *89*, 271.
56. Koh, J. Y.; Choi, D. W. *J. Neurosci. Methods* **1987**, *20*, 83.
57. Livett, B. G. *Physiol. Rev.* **1984**, *64*, 1103.
58. Moro, M. A.; López, M. G.; Gandía, L.; Michelena, P.; García, A. G. *Anal. Biochem.* **1990**, *185*, 243.